

Effects of a fluctuating water table: column study on redox dynamics and fate of some organic pollutants

A.J.C. Sinke^{a,*}, O. Dury^b, J. Zobrist^c

^a *Swiss Federal Institute for Environmental Science and Technology (EAWAG), Limnological Research Center, CH-6047 Kastanienbaum, Switzerland*

^b *Institute of Terrestrial Ecology, Soil Protection, Swiss Federal Institute of Technology (ETHZ), CH-8952 Schlieren, Switzerland*

^c *Swiss Federal Institute for Environmental Science and Technology (EAWAG), CH-8600 Dubendorf, Switzerland*

Abstract

The development of the redox conditions has been studied in an initially aerobic column filled with quartz sand coated with ferrihydrite and subjected to a fluctuating water table. The purpose of this study was to evaluate the effect of water table fluctuations on the redox dynamics and the fate of selected organic pollutants. The column that was percolated continuously with electron acceptors (O_2 , NO_3 , SO_4) and electron donors (acetate and formate), was first operated under saturated conditions resulting in the classical redox zonation. After 4 months of operation, we started to fluctuate the water level and three drainage–imbibition cycles were run each with a total cycle length of 1 month. The pulse of oxygen introduced by lowering the water table caused a partial and temporal oxidation of previously reduced species. To investigate the effect of the changing redox environment on the transport and transformation of organic pollutants, breakthrough experiments were performed with 4-nitrobenzoate and toluene as model pollutants representative for nitro-substituted and volatile aromatics, respectively. The fate of 4-nitrobenzoate and toluene was studied under saturated conditions in short pulse breakthrough experiments and evaluated using the advection–dispersion model. 4-nitrobenzoate was transformed stoichiometrically into 4-aminobenzoate caused by the reduction of the nitrogroup. The transformation rate varied with depth and with time, dropping from $15.3 \text{ nmol g}^{-1} \text{ h}^{-1}$ after the first drainage–imbibition cycle to $1.5 \text{ nmol g}^{-1} \text{ h}^{-1}$ after 4 additional months of operation. Toluene was not degraded during the first breakthrough experiment and showed a retardation factor of 2.06 which

* Corresponding author. TNO Institute of Environmental Sciences, Energy Research and Process Innovation, PO box 342, 7300 AH Apeldoorn, The Netherlands.

was ascribed to diffusion into entrapped air, originating from drainage–imbibition cycles, and to sorption to biomass. After the 24-h pre-exposure to toluene, adaptation had occurred and in later experiments toluene was degraded within the first 6 cm. These data show that in an experiment that was well-described in terms of water flow, gas flow, and initial mineral phase composition, the microbial processes induced a chemical and physical heterogeneity. An additional heterogeneity in space and time was introduced by the fluctuating water table. The ‘history’ of the column had consequences for the fate of organic pollutants and resulted in an unpredictable behaviour with respect to their transformation, transport and degradation. © 1998 Elsevier Science B.V. All rights reserved.

Keywords: Redox; Unsaturated zone; Heterogeneity; Organic pollutants

1. Introduction

In soils, there is a natural gradient in water content going from unsaturated in the top soil to fully saturated conditions at the groundwater table. In the capillary fringe above the water table, the pore volume is occupied by varying portions of water and air. This distribution of water and air has direct effects on microbial processes at a water saturation level below the field capacity, as the microbial activity can be limited by the water availability (Konopka and Turco, 1991). In laboratory systems, it was demonstrated that also the degradation of organic pollutants depended on the water saturation (Harms, 1996). For a volatile component such as naphthalene, the degradation rates increased with the enhanced effective diffusivities at lower saturation levels (Harms, 1996). In column experiments with 2,4-dichlorophenoxyacetic acid, the decreased availability of oxygen under saturated conditions was considered to be responsible for the declined degradation rates (Estrellea et al., 1993).

Little is known about the effects of fluctuations of the water table under field situations. Recently, it was demonstrated in laboratory experiments that fluctuating the water table enhanced the degradation of diesel oil (Rainwater et al., 1993). It can be expected that the dynamic regime imposed by a fluctuating water table and the resulting differences in soil aeration, not only affect the microbial and chemical reactions that organic pollutants undergo but also the transport of gases and solutes through the aquifer.

Redox conditions are likely to be influenced by the increased supply of oxygen under unsaturated conditions. The effects of the prevailing redox conditions on the degradation of organic contaminants under saturated conditions has been thoroughly investigated in the past decades. Strongly reduced conditions favour dechlorination reactions but hinder the degradation of benzene and alkylated benzenes. In contrast, the presence of oxygen supports the complete degradation of most non-halogenated aromatics (Zitomer and Speece, 1993; Bosma et al., 1996). In laboratory experiments and in waste water treatment plants, it was demonstrated that an alternating regime of aerobic–anaerobic conditions stimulated the complete mineralization of various contaminants including chlorinated compounds (Zitomer and Speece, 1993).

In addition to the effects on microbial processes, the prevailing redox conditions can also influence the chemical processes that organic pollutants undergo such as sorption

and transformation. The increased supply of organic solutes at contaminated sites commonly leads to the formation of a redox zonation in the plume of landfills going from anaerobic close to the dump-site to aerobic in the pristine aquifer (Lyngkilde and Christensen, 1992). The input in the aquifer of reduced inorganic species such as ammonium, ferrous iron, hydrogen sulfide, and methane regulates the geochemistry of the aquifer and results in a series of buffering reactions during which specific minerals are dissolved locally while others are precipitated. Examples are the dissolution of carbonates and ferric(hydr)oxides and the formation of pyrite and magnetite (Lovley, 1991a; von Gunten and Zobrist, 1993; Heron and Christensen, 1995). As a consequence of the introduction of the organic substances, the sorption behaviour of the aquifer may be altered. Especially, the sorption of hydrophobic compounds is likely to be enhanced due to the increased organic matter content and the developing biomass. Changes in the mineral composition may also affect sorption of organic and inorganic substances (Mackay et al., 1986; Barber et al., 1992). Some of the produced mineral phases such as sorbed Fe(II) species, are known to catalyse the chemical transformation of nitroaromatic compounds into the corresponding anilines (Heijman et al., 1995).

This paper reports the investigation on the effects of a fluctuating water table on microbial, chemical, and hydraulic properties that occurred in a laboratory experiment that was well-defined in terms of water flow, gas flow, and initial mineral phase composition and that lasted for 1 year. The purpose of our study was to evaluate the effect of a changing redox environment introduced by a fluctuating water table on the transport and transformation of toluene and 4-nitrobenzoate as model pollutants representative for volatile and nitrosubstituted aromatic hydrocarbons, respectively.

2. Materials and methods

2.1. Column experiments

Clean quartz sand was used with grain sizes ranging from 0.08 to 1.2 mm (Dury et al., 1998). The sand was coated with 2-line ferrihydrite ($84 \mu\text{mol g}^{-1}$) as described earlier (Scheidegger et al., 1993). A hard PVC column (length 59 cm, ID 5.3 cm) equipped with side ports with Teflon lined septa at different depths (Fig. 1), was filled with dry sand to a filling procedure that results in a homogeneous packing (Stauffer and Dracos, 1986). The gravimetrically determined porosity of the sand was 0.34 and the total pore volume 442 cm^3 . The column was carefully evacuated and flushed with N_2 to remove as much oxygen as possible. The column was slowly saturated by upward flow of artificial groundwater (AGW) which was prepared by dissolving (μM): CaCl_2 (165), NaHCO_3 (330), MgSO_4 (100), NH_4NO_3 (200), KH_2PO_4 (6.3). The AGW was flushed continuously with a gas mixture of $\text{CO}_2/\text{O}_2/\text{N}_2$ (1/1/98%). An excess of granulated marble in the medium served as carbonate buffer in combination with the 1% CO_2 in the gas phase. To sustain bacterial growth 0.5 ml l^{-1} of a trace minerals solution and 0.5 ml l^{-1} of a vitamins solution were added (Lovley and Phillips, 1988). During the experiment, the column was operated in a downflow mode and the AGW was sprinkled on top of the column using a pulsating pump and sprinkling device (Dury et al., 1998; Lehmann et al., 1998). Acetate and formate as carbon sources were added separately by

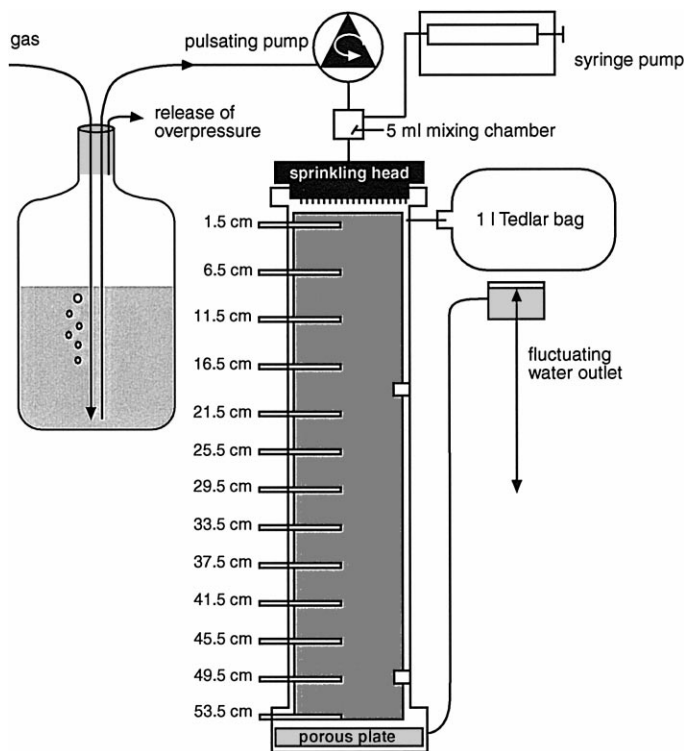


Fig. 1. Experimental set-up.

a syringe pump just before entrance in the column. Final concentrations were 1 mM for each compound. The average seepage rate during the whole experiment of 14 months was 18.8 cm d^{-1} (414 ml d^{-1}) but for some breakthrough experiments, the flow velocity was adapted. Chloride (100 mM) was used as conservative tracer to determine the transport characteristics of the system. Leachate water from a landfill near Winterthur (CH) was used as inoculum and was injected at 10-cm intervals and at the top and bottom. The column was incubated in the dark at 15°C during 14 months.

Concentration profiles in the column of nitrite, nitrate, sulfate and Fe(II) were determined regularly to follow the redox dynamics. The pore water samples were taken through the side ports from the centre of the column using 1-ml plastic or glass syringes.

To investigate the effect of the prevailing redox conditions on transport, transformation and degradation of organic contaminants, breakthrough experiments were performed in different phases of the experiment with 4-nitrobenzoate (250 or $600 \mu\text{M}$) and toluene ($75 \mu\text{M}$) that were added to AGW.

2.2. Fluctuating water level

The experiment was divided into three phases according to the differences in the imposed hydraulic regime. In phase I (4 months) the column was operated under

saturated conditions. In phase II (3 months), the water level was fluctuated and in phase III (5 months) the column was operated under saturated conditions again. In phase II, three drainage–imbibition cycles were run. The lowering of the water level was performed within 24 h and then the unsaturated conditions were maintained for 1 week. After this period, the column was imbibed again and kept saturated for 3 weeks before starting the next cycle. The height of the effluent outlet was lowered so that the water level dropped 25 cm overnight (Fig. 2). The system was kept closed and the pore space of the unsaturated zone was filled with the gas mixture that contained 1% O₂ (CO₂/O₂/N₂: 1/1/98%). The gas mixture was supplied by connecting a slightly over-pressurized Tedlar bag (1 l) to the top of the column (Fig. 1). This construction enabled us to keep the system air-tight and lower the water level without inducing an underpressure. Only for the first drainage was the water replaced by atmospheric air. After 1 week of unsaturated conditions, the water level was raised again by elevating the height of the effluent outflow. The height of the outflow was kept below the original level to prevent overpressure in the system (Fig. 2).

The water content distribution in the soil column at different stages of the experiment was modelled using the one-dimensional unsaturated flow model HYSTFLOW (Stauffer, 1996; Lehmann et al., 1998). This model is based on Richards' equation and takes into account the hysteretic capillary pressure–saturation relationship. The drainage and imbibition retention curves of the sand packing were reported elsewhere (Dury et al.,

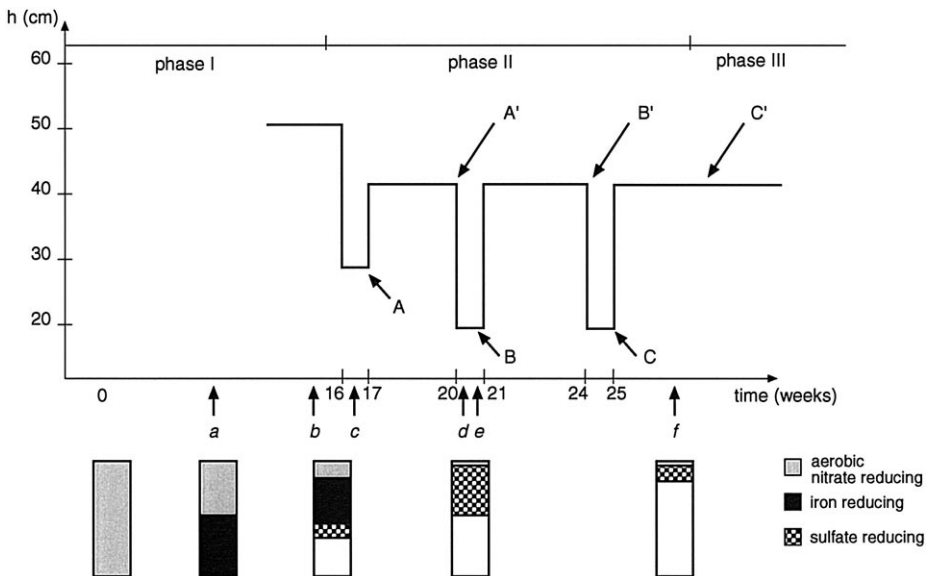


Fig. 2. (A) Schematic representation of the fluctuating pressure head lower boundary condition as a function of time. Indicated are the different phases and the different states of water saturation. h is the height measured from the bottom of the sand packing. At the x -axis the letters refer to described profiles (Fig. 3, Fig. 5 and Fig. 6). The bars represent a schematic indication of the redox conditions in the column as inferred from the profiles (Fig. 3 and Fig. 6).

1998). The hydraulic permeability at full saturation was 1.6 cm min^{-1} , as determined from extrapolation of the data of Dury. The modelling was performed using a constant flux upper boundary condition set to a value of $0.0125 \text{ cm min}^{-1}$ and a fluctuating pressure head boundary as depicted in Fig. 2.

2.3. Analytical methods

Chloride was measured electrochemically with a Chlorocounter (Marius, Nieuwegein, NL). Nitrite, nitrate, and sulfate were measured by ion chromatography, a conductivity detector (IC 690, Metrohm, Herisau, CH), PRP-X100 column, and an aqueous eluent with phthalic acid (2 mM) and acetone (10%).

Iron in solution was measured spectrophotometrically (562 nm) after reaction with Ferrozine (Stookey, 1970). The total amount of iron was measured as Fe(II) after reduction with hydroxylamine hydrochloride (0.25 M).

4-Nitrobenzoate, 4-aminobenzoate and toluene were determined with HPLC and UV detection. Benzoates were measured at 254 nm using an RP-18 reversed phase column (Merck, Darmstadt, Germany) and an aqueous eluent (1 ml min^{-1}) with 40% methanol and 1% phosphoric acid. Toluene was measured at 206 nm using a RP-8 column (Merck, Darmstadt, Germany) and an aqueous eluent with 80% methanol (1 ml min^{-1}).

2.4. Data analysis

The advective–dispersive model was fitted to the breakthrough curves using the computer program CXTFIT (Parker and Van Genuchten, 1984) or CXTFIT version 2.0 (Toride et al., 1995). This program allows to estimate transport parameters such as pore water velocity (V , cm min^{-1}), the retardation factor (R , –) and dispersion coefficient (D , $\text{cm}^2 \text{ min}^{-1}$) by a non-linear least squares inversion method. For the chloride breakthrough curves the retardation factor was fixed at a value of 1 and V and D were fitted. For the breakthrough curves of 4-nitrobenzoate and toluene, the fitted values for V and D were used as input parameters and inverse modelling was used to estimate the retardation factor (R).

3. Results and discussion

3.1. Development of a redox zonation

The development of the redox conditions with time was inferred from the changes in concentration profiles of nitrate and sulfate (Fig. 3). At the start of the experiment, the whole column was aerobic. After 4 weeks of operation, nitrate was no longer detected in the effluent (data not shown). After 12 weeks, most nitrate was consumed within the first 2 cm and the concentration dropped from 200 to $30 \mu\text{M}$. However, the nitrate reduction rate between 2 and 20 cm depth was low and nitrate could still be detected at a depth of 21.5 cm (Fig. 3A). Nitrite was never detected in the pore water. The sulfate concentration dropped slightly in the first 10 cm but did not decrease further with depth.

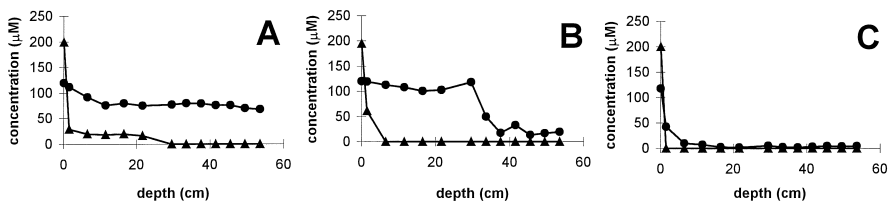


Fig. 3. Development of the redox conditions during the experiment with (▲) nitrate and (●) sulfate concentration. (A) Initial profiles at time *a* (Fig. 2) with aerobic and nitrate reducing conditions throughout the column; (B) profiles at time *b* with distinct redox zonation; (C) profiles at time *f* in which microbial redox processes are comprised in the active top layer.

During phase I, the column gradually turned black and in week 15, a clear redox zonation had developed (Fig. 3B). From the concentration profiles, we concluded that nitrate reduction dominated in the top 5 cm. The sulfate concentrations did not change much in the top 30 cm but dropped significantly between 30 and 40 cm depth indicating the presence of a sulfate reducing zone. Presumably between 5 and 30 cm depth, iron reduction dominated the system. However, the concentration profiles of Fe(II) did not reveal any distinct Fe(II) production zones and the measured pore water concentrations of Fe(II) varied between 10 and 170 μM in the whole column without clear trends. It can be assumed that part of the produced Fe(II) reacted further immediately and formed solid phases such as FeCO_3 , FeS and FeS_2 (von Gunten and Zobrist, 1993) or readsorbed to the Fe(III) hydroxide forming magnetite (Fe_3O_4) (Lovley, 1991b). The formation of magnetite was indicated by the black colour that was formed above the sulfate reducing zone. Also, the sulfate reducing zone itself was black due to FeS produced. Initially, the two dark zones that had slightly different colour intensities were spatially separated by a zone with a lighter colour but the observed difference disappeared with the extension of the zones.

Phase II was the period during which the water level was fluctuated (see below). Finally, in phase III, an active biofilm had developed on top of the column in which oxygen, nitrate, and sulfate were rapidly depleted (Fig. 3C).

3.2. Water table fluctuations and redox hysteresis

The imposed water level fluctuations had a relatively small amplitude and therefore, the lower part of the column remained fully water-saturated during the whole experiment. During the first drainage period, the capillary fringe was located in the upper 10 cm of the column. During the second and third drainage period the uppermost 25 cm of the column were unsaturated as indicated by the modelled water distribution (Fig. 4). The water content in the soil column at different stages of the experiment varied between 0.34 and 1.0 (Fig. 4). The exact final saturation in the imbibed state (*A'*, *B'*, and *C'*, Fig. 2) was not determined experimentally so the modelled curves could not be verified. The column was fully saturated (1.0) at the beginning of the experiment as the sand packing had been imbibed by upward flow with a free outlet. Between steps A and *A'*, the unsaturated column was re-saturated with water but during this process part of

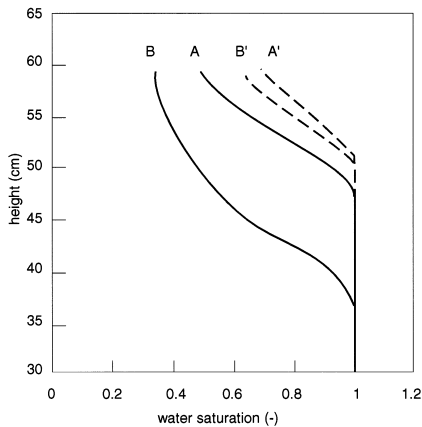


Fig. 4. Modelled water content profiles at the end of each state of the fluctuations (C and C' are identical to B and B'). The calculated amounts of air volume (cm^3) for each state were A: 43.2; A': 17; B(=C): 132.5; B'(=C'): 23.8.

the air remained entrapped as bubbles or small ganglia within the water phase. Therefore, the water saturation at state A' is somewhat lower than 1.0. The volume of air that was present in the column in the successive states was estimated from Fig. 4 and compared to the main drainage curve given by Dury et al. (1998) for the same porous medium. Because of the uncertainty of the full saturation (< 1), the air content is probably slightly underestimated but since the fluctuations remained in the domain of high water saturation, the approximation should be reliable.

During the first drainage, the pore space was filled with air and this introduction of oxygen resulted in an oxidation of the reduced sulfur species as apparent from the ten-fold increase in the sulfate concentration between the influent ($120 \mu\text{M}$) and the pore water concentration at 16.5 cm ($1030 \mu\text{M}$) (Fig. 5). The oxidation was very rapid and the generated sulfate was transported downwards with the percolating water. As a result of the drop in water level the black colour disappeared in the upper part of the column leaving the sand greyish-yellow. The oxidation of Fe(II) and the formation of fresh Fe(III)(hydr)oxide, could not be ascertained as we did not want to dissect the

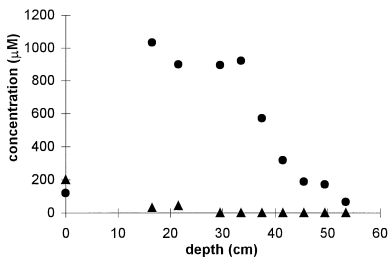
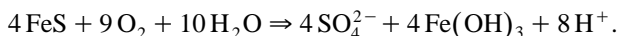
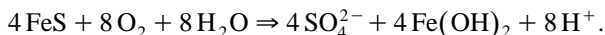


Fig. 5. Profiles of (▲) nitrate and (●) sulfate in a column with an unsaturated top layer 6 h after lowering of the water level in the column at time c (Fig. 2).

column. As 43.2 cm^3 of air corresponding to 0.4 mmol O_2 entered the column, 0.18 mmol of sulfate and Fe(OH)_3 could have been generated during this drainage according to:



In case that the oxidation was incomplete, slightly more sulfate would have been produced (0.2 mmol sulfate per 0.4 mmol oxygen):



We estimated the amount of sulfate produced in the column by integration of the measured concentrations at different depth and correcting for the flow velocity. Almost all of the potentially produced sulfate was recovered in the column after 10 h (Fig. 5) and apparently little had been reduced by sulfate-reducing bacteria.

During the second drainage, the entrance of gas phase was larger (132.5 cm^3) but as the gas-mixture contained only 1% O_2 , the increase in sulfate concentration was less pronounced (Fig. 6A). This time the integrated amount of sulfate present in the column of 0.06 mmol was higher than the calculated amount that could have been produced by oxidation of reduced sulfur species: 0.03 mmol (132.5 cm^3 , 1% O_2 gives 0.06 mmol O_2). However, it is difficult to distinguish between the produced sulfate and the sulfate that entered the column with the influent. After 3 days, the major part of the sulfate had been washed-out (Fig. 6B). The sulfate reducing zone had moved further upwards as compared to the profile in Fig. 3B and now all sulfate was reduced in the upper 30 cm of the column.

During phase II, the amount of Fe(II) that was washed-out of the system increased remarkably. The average effluent concentration rose from $26 \mu\text{M}$ in phase I to $73 \mu\text{M}$ during phase II and decreased again to $51 \mu\text{M}$ in phase III. From the measured data, it cannot be concluded which processes were responsible for the increased production of Fe(II) during the water table fluctuations. From the literature, it can be deduced that several processes could have contributed to the observed washout of Fe(II) (Davison, 1991; von Gunten and Zobrist, 1993; Postma and Jakobsen, 1996): first, by an increased iron reduction, secondly, by an accelerated reductive dissolution of ferrihydrite driven by the production of sulfide, and thirdly, by a local drop of the pH caused by the oxidation of FeS resulting in an increased solubility of FeS. It can be expected that the first two processes would have resulted in an increased precipitation of FeCO_3 and FeS in the column and only the latter process could lead to an increased solubility of iron

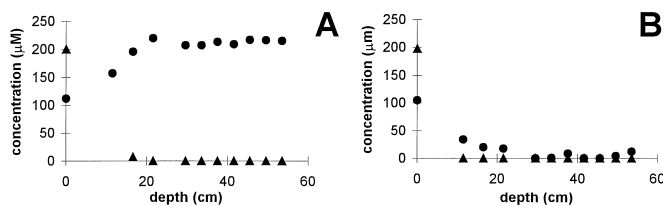


Fig. 6. (A) Profiles of (▲) nitrate and (●) sulfate in a column with an unsaturated top layer after lowering of the water level at time *d* (Fig. 2) and profiles 3 days later at time *e*.

minerals and can be held responsible for the increased washout of Fe(II) from the system.

After the third drainage–imbibition cycle, the distinct iron reduction zone had disappeared and the sulfate reducing zone had moved upward (data not shown). The balance between iron and sulfate reducers is governed by environmental conditions like the pH and stability of the iron (hydr)oxides present (Postma and Jakobsen, 1996). The continued washout of iron indicates that iron reduction still proceeded but probably the iron reducing bacteria will be gradually out competed in our column because of the decreasing availability of iron.

3.3. Transport and transformation of 4-nitrobenzoate

After 20 weeks, just before the second drainage–imbibition cycle, a breakthrough experiment with chloride and 4-nitrobenzoate was performed (Fig. 7). In the initial phase of the breakthrough, all nitrobenzoate was stoichiometrically transformed into aminobenzoate (Fig. 7B). Only in a later stage of the pulse did the transformation rate decline and 4-nitrobenzoate start to break through.

The integrated amount of 4-nitro and 4 aminobenzoate in the effluent equalled the input of 4-nitrobenzoate indicating that under the prevailing conditions, only transformation occurred and no degradation. The inverse modelling with CXTFIT of the sum of both substituted benzenes, taking the V and D fixed at the values calculated from the chloride breakthrough, resulted in a retardation factor of 1.007 ($R^2 = 0.99$). This value

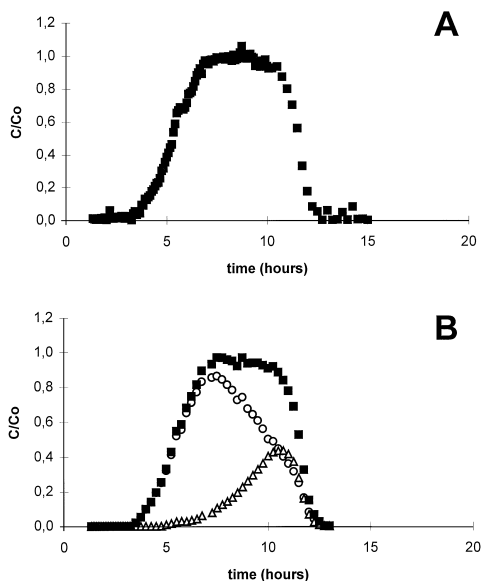


Fig. 7. Breakthrough curves of nitrobenzoate carried out after the first drainage and imbibition cycle (Fig. 2) with nitrobenzoate (Δ), aminobenzoate (\circ), and total benzoates (\blacksquare).

does not deviate significantly from 1 implying that both substituted benzoates did not sorb. Undissociated nitroaromatic compounds can be expected to be strongly retarded in soils with clay minerals to which they sorb specifically (Haderlein and Schwarzenbach, 1993; Fesch et al., 1998). The produced amino-compounds can sorb in soils with complex organic matter (such as humic acids) where bound-residue formation occurs. As in our column, the benzoates were fully dissociated and no complex organic matter was present, both nitro- and amino-compounds were transported without retardation.

By comparing successive hourly profiles of 4-nitro and 4-aminobenzoate with those of chloride, we estimated the initial transformation rate that occurred during the passage of the moving front of nitrobenzoate through the column. We also calculated the long-term transformation rate that occurred afterwards and appeared to be approximately constant. Both the initial and the long-term reduction rate were spatially heterogeneous (Table 1). The initial transformation rate appeared to be lower in the upper 15 cm of the column than in the bottom part 15.2 and 24.2 $\text{nmol g}^{-1} \text{h}^{-1}$, respectively. The long-term transformation rate was somewhat slower: 12.7 and 15.3 $\text{nmol g}^{-1} \text{h}^{-1}$ in the top and bottom part, respectively. The transformation rate of the nitrogroup in the middle part of the column deviated clearly and was much lower: 4.3 $\text{nmol g}^{-1} \text{h}^{-1}$.

After 9 months, in phase III, a second breakthrough of 4-nitrobenzoate was recorded which deviated considerably from the first measurement (Fig. 8). In this phase, the column had an active top layer in which all redox processes were comprised. Only minor amounts of 4-nitrobenzoate were transformed into 4-aminobenzoate. The long-term rate of transformation of the nitro-group was 1.5 $\text{nmol g}^{-1} \text{h}^{-1}$ almost a factor 10 lower than in the first experiment.

Heijman et al. (1995) reported a stoichiometric transformation of nitroaromatic compounds into the corresponding anilines and hypothesized that the reaction with sorbed Fe(II) resulted in the abiotic reduction of the nitrogroup and the regeneration of Fe(III). In congruence to this, the spatial differences in both the initial and long-term rate in our column could be caused by the amount of sorbed Fe(II) and its speciation. The high initial transformation rates in the first experiment could be due to the instantaneous chemical reaction between the nitrogroup and the sorbed Fe(II) that had been stored in the column during the preceding 4 months. In the second experiment, the initial transformation rates were much lower, which can be explained by the fact that much of the iron had been washed-out.

Table 1

Initial and long-term reduction rate of 4-nitrobenzoate under saturated conditions in different zones of the sand column after 20 weeks of operation

Depth (cm)	Saturation characteristics during drained state	Reduction rate of 4-nitrobenzoate ($\text{nmol g}^{-1} \text{h}^{-1}$)	
		Initial	Long-term
0–15	unsaturated part, saturation < 0.4	15.2	12.7
15–30	capillary fringe, saturation 0.4–1.0	15.2	4.3
30–59	saturated part, saturation 1.0	24.2	15.3

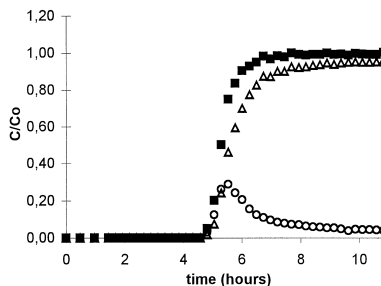


Fig. 8. Breakthrough curves of nitrobenzoate carried out after three drainage imbibition cycles (phase III, Fig. 2) with nitrobenzoate (Δ), aminobenzoate (\circ), and total benzoates (\blacksquare).

The decrease in the transformation rate with time during the breakthrough might be caused by the exhaustion of Fe(II) caused by its oxidation by the passing nitro-groups. The fact that in both experiments the transformation lasted also on the long run, suggests that the Fe(II) is regenerating continuously. Heijman et al. (1995) hypothesized the indirect involvement of iron-reducing bacteria that reduced the formed Fe(III) and thereby regenerated Fe(II) which is necessary for the chemical reaction with the nitrogroups. The zone of extremely low long-term reactivity in the middle part of the column coincides with the zone where the capillary fringe was located under unsaturated conditions. Apparently, the fluctuating water regime induced changes in chemistry and microbiology in this zone leading to lower transformation rates.

3.4. Transport and degradation of toluene

One week after the second breakthrough experiment with 4-nitrobenzoate, the first experiment with toluene was performed under saturated conditions (phase III). The concentration profiles of chloride, measured at 1 h intervals during the combined breakthrough of chloride and toluene, were used in an inverse modelling procedure with CXTFIT to estimate the dispersion coefficient and pore water velocity in the column (Fig. 9A). The fitted values for the pore water velocity based on the effluent concentrations underestimated the actual value by 13%. This underestimation is caused by the fact that during each sampling, 9 ml of pore water were extracted from the column which is almost 3% of the total pore water volume. The breakthrough of $75 \mu\text{mol l}^{-1}$ toluene was complete after 24 h and no degradation was observed (Fig. 9B). The toluene was clearly retarded and a retardation factor of 1.5 was calculated taking the fitted values for the pore water velocity and dispersion coefficient as fixed. The comparison of the measured toluene concentrations with the ones estimated from the inverse modelling (Fig. 10) demonstrated that the values were considerably lower in the upper part and higher in the lower part of the column. When the same approach was applied to the toluene data of the upper 11.5 cm only, a retardation of 2.06 was calculated, indicating that the retardation in the top of the column was much higher and that in the lower part hardly any retardation occurred. The strong retardation in the upper part of the column

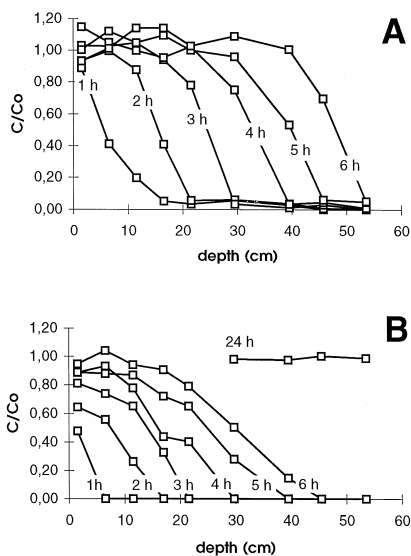


Fig. 9. Profiles of chloride (A) and toluene (B) in a breakthrough experiment carried out during phase III (Fig. 2).

could be caused by (i) the presence of a thick biofilm with a high organic matter content or (ii) the presence of trapped air bubbles in the upper layer of the column. An organic matter fraction (f_{oc}) of 0.52% is necessary to explain the high retardation of toluene. This estimation was made taking K_{ow} for toluene of 490 (Schwarzenbach et al., 1983) and K_d of 0.22, which was calculated from the retardation constant of 2.06, and by using the relationship $K_d = 0.49 f_{oc} \times K_{ow}^{0.72}$ (Schwarzenbach and Westall, 1981). Such an organic matter content is relatively high—the original f_{oc} of the sand used was only 0.1%. Hence, the observed retardation of toluene in the top layer is probably also due to partitioning into trapped air of the formerly unsaturated zone. When sorption to organic matter is neglected, an air volume of 27%, was needed to explain the observed retardation. The estimation was made as follows: the retardation in unsaturated systems

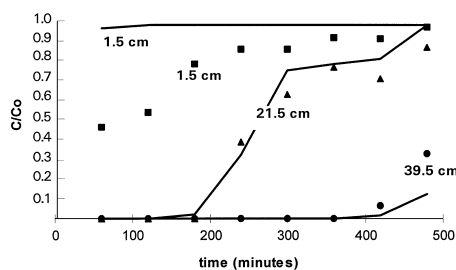


Fig. 10. Breakthrough of toluene at different depths. Lines are results of the parameter estimation with CXTFIT 2.0.

is due to sorption to the solid phase and to partitioning into the immobile, and discontinuous gas phase. The retardation coefficient is then described as

$$R = 1 + \frac{\rho_b}{\vartheta_w} K_d + \frac{\vartheta_g}{\vartheta_w} H$$

where ρ_b is the bulk density (M l^{-3}), K_d is the distribution coefficient with the solid phase ($\text{l}^3 \text{M}^{-1}$), ϑ_w is the fraction of water volume ($\text{l}^3 \text{l}^{-3}$), ϑ_g is fraction of gas volume ($\text{l}^3 \text{l}^{-3}$) and H is the Henry constant (–). When the sorption to organic matter is neglected ($K_d = 0$) and assuming a Henry constant of 0.26, a gas volume of 27% results in a retardation factor of 2.06. This 27% is significantly above the expected range after the applied drainage–imbibition cycles. The amount of trapped air at state B' and C' (Fig. 4) is 23.8 cm^3 in the top 20 cm of the column (pore volume $20/60 \times 442 = 147 \text{ cm}^3$) resulting in an air volume of 16%.

In a second breakthrough experiment with toluene ($60 \mu\text{M}$) which was performed 1 week later, the amount of acetate and formate was decreased to $200 \mu\text{M}$. Under these conditions, toluene did not break through but was degraded within the first 6 cm. Unfortunately, the number of data points did not permit to do any fitting with a CXTFIT routine that included degradation. To clarify whether during the first breakthrough the toluene degradation had been prevented by an oversupply of carbon, we increased the concentration of acetate and formate again in a third and fourth breakthrough experiment. However, in later experiments, toluene never broke through again, indicating that toluene was readily degraded. A lag-phase occurs often before degradation of organic contaminants starts (van der Meer et al., 1992). Generally, this lag-phase can be attributed to either (1) the increase in number of bacteria capable to degrade the compound, (2) the induction of specific enzymes in already present bacteria or (3) molecular mechanisms such as mutations and exchange of DNA that result in the development of a bacterial population with altered characteristics. The last mechanism can be relevant when long lag periods are observed. It is likely that the used inoculum from the waste deposit site contained toluene degraders because this site is heavily contaminated with polyaromatic hydrocarbons (T. Bosma and L. Spack, personal communication). The short 24-h exposure to toluene might have resulted in an increased biomass of toluene degraders or might have activated the enzyme system of present bacteria and a second pulse of toluene was degraded efficiently. Also, Jin et al. (1994) reported that pre-exposure of the soil to toluene greatly increased the rate of degradation. The transport of toluene and its degradation apparently depends on the 'history' of the column and is hard to predict.

4. Conclusions

From our results, it became clear that the redox conditions in a sand column with a fluctuating water table were not in equilibrium but subject to spatial and temporal variation. The microbial processes in the column that was well-defined in terms of water flow, gas flow, and initial mineral phase, resulted in a heterogeneity that had consequences for the fate of organic pollutants.

We demonstrated that the transformation rate of nitrobenzoate being a model compound for nitrosubstituted aromatics, varied with depth and with time with rates dropping from 15–20 nmol g⁻¹ h⁻¹ in the first experiment carried out after 20 weeks to 1.5 nmol g⁻¹ h⁻¹ in the experiment carried out after 32 weeks. The transport of toluene chosen as a model compound for volatile organics was studied under saturated conditions after three drainage–imbibition cycles. In the first breakthrough experiment, toluene was not degraded. Toluene was retarded ($R = 2.06$) by sorption to the trapped air present in the formerly unsaturated zone and by sorption to the developed thick biofilm. Repeated pulses of toluene resulted in an adaptation of the microbial community and in a complete degradation.

Also, in natural environments, redox conditions and the fraction of gas volume are not in steady state but vary spatially and temporally in an aquifer. Consequently, the fate of an organic pollutant in an aquifer may change also with time and location.

Acknowledgements

This work is part of the OPUS-IA project of the Swiss Federal Institutes. The authors want to thank H.-P. Läser and B. Studer for constructing the column and E. Grieder for help with IC measurements. H. Harms, T. Bosma, and F. Stauffer are thanked for discussions. CXTFIT 2.0 was a kind gift of R. Van Genuchten.

References

- Barber, L.B.I., Thurman, E.M., Runnells, D.D., 1992. Geochemical heterogeneity in a sand and gravel aquifer: effect of sediment mineralogy and particle size on the sorption of chlorobenzenes. *J. Contam. Hydrol.* 9, 35–54.
- Bosma, T.N.P., Ballemans, E.M.W., Hoekstra, N.K., te Welscher, R.A.G., Smeenk, J.G.M.M., Schraa, G., Zehnder, A.J.B., 1996. Biotransformation of organics in soil columns and an infiltration area. *Ground Water* 34 (1), 49–56.
- Davison, W., 1991. The solubility of iron sulphides in synthetic and natural waters at ambient temperature. *Aquat. Sci.* 53 (4), 309–329.
- Dury, O., Fischer, U., Schulin, R., 1998. Dependence of hydraulic and pneumatic characteristics of soils on a dissolved organic compound. *J. Contam. Hydrol.* 33, 39–57.
- Estrellea, M.R., Brusseau, M.L., Maier, R.S., Pepper, I.L., Wierenga, P.J., Miller, R.M., 1993. Biodegradation, sorption, and transport of 2,4-dichlorophenoxyacetic acid in saturated and unsaturated soils. *Appl. Environ. Microbiol.* 59, 4266–4273.
- Fesch, C., Lehmann, P., Haderlein, S.B., Hinz, C., Schwarzenbach, R., Flüher, H., 1998. Effect of water content on solute transport in a porous medium containing reactive micro-aggregates. *J. Contam. Hydrol.* 33, 211–230.
- Haderlein, S.B., Schwarzenbach, R.P., 1993. Adsorption of substituted nitrobenzenes and nitrophenols to mineral surfaces. *Environ. Sci. Technol.* 27, 316–326.
- Harms, H., 1996. Bacterial growth on distant naphthalene diffusing through water, air and water saturated and nonsaturated porous media. *Appl. Environ. Microbiol.* 62, 2286–2293.
- Heijman, C.G., Grieder, E., Holliger, C., Schwarzenbach, R.P., 1995. Reduction of nitroaromatic compounds coupled to microbial iron reduction in laboratory aquifer columns. *Environ. Sci. Technol.* 29 (3), 775–783.
- Heron, G., Christensen, T.H., 1995. Impact of sediment-bound iron on redox buffering in a landfill leachate polluted aquifer (Vejen, Denmark). *Environ. Sci. Technol.* 29, 187–192.

- Jin, Y., Streck, T., Jury, W.A., 1994. Transport and biodegradation of toluene in unsaturated soil. *J. Contam. Hydrol.* 17, 111–127.
- Konopka, A., Turco, R., 1991. Biodegradation of organic compounds in vadose zone and aquifer sediments. *Appl. Environ. Microbiol.* 57, 2260–2268.
- Lehmann, P., Stauffer, F., Hinz, C., Dury, O., Flühler, H., 1998. Effect of hysteresis on water flow in a sand column with a fluctuating capillary fringe. *J. Contam. Hydrol.* 33, 81–100.
- Lovley, D.R., 1991a. Dissimilatory Fe(III) and Mn(IV) reduction. *Microbiol. Rev.* 55 (2), 259–287.
- Lovley, D.R., 1991. Magnetite formation during microbial dissimilatory iron reduction. In: Frankel, R.B., Blakemore, R.P. (Eds.), *Iron Biominerals*. Plenum, New York, pp. 151–166.
- Lovley, D.R., Phillips, E.J.P., 1988. Novel mode of microbial energy metabolism: organic carbon oxidation coupled to the dissimilatory reduction of iron or manganese. *Appl. Environ. Microbiol.* 54, 1472–1480.
- Lyngkilde, J., Christensen, T.H., 1992. Redox zones of a landfill leachate pollution plume. *J. Contam. Hydrol.* 10, 291–307.
- Mackay, D.M., Ball, W.P., Durant, M.G., 1986. Variability of aquifer sorption properties in a field experiment on groundwater transport of organic solutes: methods and preliminary results. *J. Contam. Hydrol.* 1, 119–132.
- Parker, J.C., Van Genuchten, M.T., 1984. Determining transport parameters from laboratory and field tracer experiments. Virginia Agricultural Experiment Station.
- Postma, D., Jakobsen, R., 1996. Redox zonation: equilibrium constraints on the Fe(III)/SO₄-reduction interface. *Geochim. Cosmochim. Acta* 60 (17), 3169–3175.
- Rainwater, K., Mayfield, M.P., Heintz, C., Claborn, B.J., 1993. Enhanced in situ biodegradation of diesel fuel by cyclic vertical water table movement: preliminary studies. *Water Environ. Res.* 65, 717–725.
- Scheidegger, A., Borkovec, H., Stichter, H., 1993. Coating of silica sand with goethite: preparation and analytical identification. *Geoderma* 58, 43–65.
- Schwarzenbach, R.P., Westall, J., 1981. Transport of nonpolar organic compounds from surface water to groundwater. *Environ. Sci. Technol.* 15, 1360–1367.
- Schwarzenbach, R.P., Giger, W., Hoehn, E., Schneider, J.K., 1983. Behavior of organic compounds during infiltration of river water to ground water: field studies. *Environ. Sci. Technol.* 17, 472–479.
- Stauffer, F., 1996. Hysteretic unsaturated flow modelling. *Hydroinformatics '96*, Balkema, pp. 589–595.
- Stauffer, F., Dracos, T., 1986. Experimental and numerical study of water and solute infiltration in layered porous media. *J. Hydrol.* 84, 9–34.
- Stookey, L.L., 1970. Ferrozine—a new spectrophotometric reagent for iron. *Anal. Chem.* 42, 779–781.
- Toride, N., Leij, F.J., Van Genuchten, M.T., 1995. The CXTFIT code for estimating transport parameters from laboratory or field tracer experiments, Version 2.0. US Salinity Laboratory.
- van der Meer, J.R., De Vos, W.M., Harayama, S., Zehnder, A.J.B., 1992. Molecular mechanisms of genetic adaptation to xenobiotic compounds. *Microbiol. Rev.* 56, 677–694.
- von Gunten, U., Zobrist, J., 1993. Biogeochemical changes in groundwater–infiltration systems: column studies. *Geochim. Cosmochim. Acta* 57, 3895–3906.
- Zitomer, D.H., Speece, R.E., 1993. Sequential environments for enhanced biotransformation of aqueous contaminants. *Environ. Sci. Technol.* 27, 226–244.